

Entrance-channel effects on the average angular momentum of compound nuclei produced in fusion reactions

C. H. Dasso

The Niels Bohr Institute, Blegdamsvej 17, DK-2100 Copenhagen Ø, Denmark

S. Landowne

Technische Universität München, D-8046 Garching, West Germany

(Received 5 March 1985)

Haas *et al.* recently observed a strong entrance-channel dependence in the angular momentum content of compound nuclei produced in fusion reactions. We explain the origin of these effects and analyze the cases of $^{16}\text{O} + ^{144}\text{Nd}$, $^{37}\text{Cl} + ^{123}\text{Sb}$, $^{64}\text{Ni} + ^{96}\text{Zr}$, and $^{80}\text{Se} + ^{80}\text{Se}$ presented by Haas *et al.*

In a recent Letter Haas *et al.*¹ reported for the first time on measurements of the average angular momentum \bar{l} produced in a series of different reactions leading to the same compound nucleus. It was observed that \bar{l} depends sensitively on the asymmetry of the entrance channel. In this Brief Report we explain this dependence and point out some additional general features of the compound nuclear spin distributions.

In an earlier paper we emphasized the important way in which coupling interactions between two colliding nuclei enhance the probability for large angular momentum fusion reactions near the Coulomb barrier.² This can be seen explicitly by using the approximate solution of the general barrier penetration problem given in Ref. 3. Within this framework the fusion cross section for a partial wave l at the center of mass energy E may be written as

$$\sigma_l(E) = \frac{\hbar^2 \pi}{2\mu E} \sum_i P_i \frac{2l+1}{1 + \exp[V_b + l(l+1)\hbar^2/2\mu r_b^2 + \lambda_i - E]/\epsilon]}$$

where μ is the reduced mass, V_b and r_b are the height and radius of the potential barrier, and the parameter ϵ is a measure of the barrier thickness. This equation generalizes the familiar parabolic barrier penetration model by introducing a weighted average over transmission functions for a collection of effective barriers. The shifts λ_i and weights P_i are obtained from diagonalizing the coupling matrix at the position of the barrier.

Using the substitutions $(2l+1) \rightarrow 2l$ and $l(l+1) \rightarrow l^2$ and treating l as a continuous variable, the normalized spin distribution is ($V_i \equiv V_b + \lambda_i$),

$$\rho(l) = \frac{\hbar^2 \sum_i P_i \{1 + \exp[(V_i + l^2 \hbar^2/2\mu r_b^2 - E)/\epsilon]\}^{-1}}{\mu r_b^2 \epsilon \sum_i P_i \ln\{1 + \exp[(E - V_i)/\epsilon]\}}$$

We are primarily interested here in the first moment \bar{l} of this distribution, which represents the average angular momentum content of the compound nuclear system.

While the function $\rho(l)$ depends on the coupling interaction and the energy E in a complicated way, its general qualitative features can be easily understood. The distribution of effective barriers is centered at V_b but generally extends more towards higher energies due to the predominance of negative Q -value reaction channels.³ The relevant weights define in any case a characteristic range of barrier heights

which we indicate by $2F$, where F is a measure of the total coupling strength. It is interesting to note that the standard quantal tunneling can also be interpreted in this way, by associating the diffuseness parameter ϵ with a modulation of the barrier height by about 4ϵ . The striking effects of the coupling on the subbarrier fusion cross section and on the near-barrier compound nucleus spin distribution are due to the fact that F is considerably larger than 2ϵ for heavy colliding systems.^{3,4}

In the higher energy range, where $E > V_b + F$, the spin distribution approaches a triangular form. The average angular momentum is approximately given by the classical limit

$$\bar{l} \approx \frac{2}{3} \sqrt{2\mu r_b^2 (E - V_b)/\hbar^2}$$

which is independent of the coupling interaction.

There is also a unique quantal limit, independent of the coupling strength, at low energies $E < V_b - F$. In this case the distribution is independent of the bombarding energy and is given by

$$\rho(l) \approx -\frac{d}{dl} (e^{-l/a^2})$$

where $a^2 \equiv 2\mu r_b^2 \epsilon/\hbar^2$. The corresponding average value of the angular momentum becomes a constant:

$$\bar{l} = \frac{\sqrt{\pi}}{2} a \approx \frac{2}{3} \sqrt{2\mu r_b^2 (2\epsilon)/\hbar^2}$$

A simple general expression cannot be given for the intermediate energy regime $V_b - F < E < V_b + F$, where the coupling interaction is effective. However the curve $\bar{l}(E)$ smoothly interpolates between the two limiting situations. A rough estimate for $E \sim V_b$ is

$$\bar{l} \approx \frac{2}{3} \sqrt{2\mu r_b^2 (F)/\hbar^2}$$

which, compared with the preceding expression, exhibits the important effect of the coupling.

The above results give a clear overview of the energy dependence of the average angular momentum. If different entrance-channel configurations are used in order to produce the same compound nucleus, the values of \bar{l} will essentially scale with the square root of the reduced masses. Thus strong differences will be noted between the symmetric and most asymmetric configurations. This is the basic explanation of the effects observed by Haas *et al.*¹

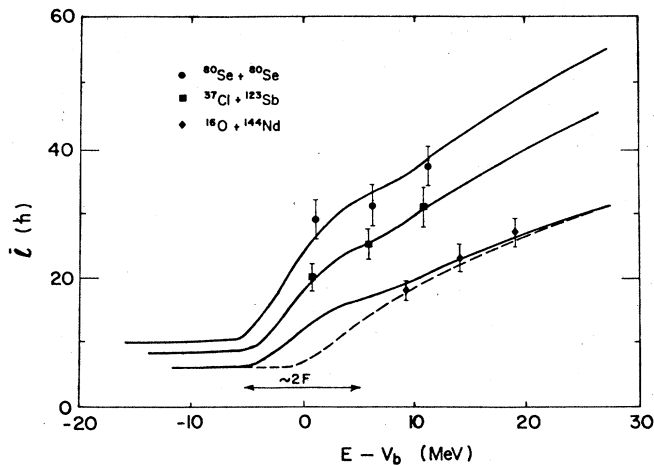


FIG. 1. Average angular momentum for the fusion reactions $^{80}\text{Se} + ^{80}\text{Se}$ (\bullet), $^{37}\text{Cl} + ^{123}\text{Sb}$ (\blacksquare), and $^{16}\text{O} + ^{144}\text{Nd}$ (\blacklozenge). The experimental points are from Ref. 1. The dashed curve is a no-coupling calculation.

The interpretation of the measurements in Ref. 1 is, however, more complicated because the bombarding energies were chosen to give fixed excitation energies of the composite system. These generally correspond to different energies with respect to the barriers. To clarify this point we have made calculations using the simplest representation of a barrier modulation of range $2F$, namely, a symmetric two-barrier distribution at $V_b \pm F$. For heavy systems $F \approx 5$ MeV,⁵ while the barrier parameters V_b , r_b , and ϵ can be estimated from systematics.⁶ The curves in Fig. 1 show the values of \bar{l} for the $^{16}\text{O} + ^{144}\text{Nd}$, $^{37}\text{Cl} + ^{123}\text{Sb}$, and $^{80}\text{Se} + ^{80}\text{Se}$

TABLE I. Barrier parameters and coupling strengths.

$a + A$	V_b (MeV)	r_b (fm)	ϵ (MeV)	F (MeV)
$^{16}\text{O} + ^{144}\text{Nd}$	62	10.6	0.69	4
$^{37}\text{Cl} + ^{123}\text{Sb}$	102	11.2	0.60	4
$^{64}\text{Ni} + ^{96}\text{Zr}$	133	11.5	0.56	5
$^{80}\text{Se} + ^{80}\text{Se}$	137	11.5	0.55	5

fusion reactions calculated using the parameters listed in Table I. The results for $^{64}\text{Ni} + ^{96}\text{Zr}$ fall between those of $^{80}\text{Se} + ^{80}\text{Se}$ and $^{37}\text{Cl} + ^{123}\text{Sb}$ but for the sake of clarity they have not been included in the figure.

Plotting \bar{l} as a function of the energy with respect to the barrier clearly brings out the effects of different initial configurations. The maximum values occur for the symmetric case. However, a slightly asymmetric combination with a strong coupling could lead to higher \bar{l} values in the barrier region.

The figure also shows that requiring equal excitation energies for the compound nucleus forces the bombarding energy to be outside the barrier region for the $^{16}\text{O} + ^{144}\text{Nd}$ case. Here the coupling interaction has no significant effect on the value of \bar{l} , as illustrated by the no-coupling limit shown by the dashed curve. As far as the overall trends in the data are concerned, the coupling effect is only apparent for the lowest energy points near $E - V_b \approx 0$. In general, the effects of the couplings would be more pronounced for the higher moments of the spin distributions.

One of us (S.L.) has been supported by a grant of the Bundesministerium für Forschung und Technologie, Federal Republic of Germany.

¹B. Haas, G. Duchêne, F. A. Beck, T. Byrski, C. Gehringer, J. C. Merdinger, A. Nourredine, V. Rauch, J. P. Vivien, J. Barrette, S. Tobbeche, E. Bozek, J. Styczen, J. Keinonen, J. Dudek, and W. Nazarewicz, Phys. Rev. Lett. **54**, 398 (1985).

²S. Landowne and C. H. Dasso, Phys. Lett. **138B**, 32 (1984).

³C. H. Dasso, S. Landowne, and A. Winther, Nucl. Phys. **A407**, 221 (1983).

⁴C. H. Dasso, S. Landowne, and A. Winther, Nucl. Phys. **A405**, 381 (1983).

⁵R. A. Broglia, C. H. Dasso, S. Landowne, and G. Pollarolo, Phys. Lett. **133B**, 34 (1983).

⁶L. C. Vaz, J. M. Alexander, and G. R. Satchler, Phys. Rep. **69**, 373 (1981).